NEW MULTI-CARRIER DEMODULATION METHOD APPLIED TO GEARBOX VIBRATION ANALYSIS

Elisa Hubert[1,2], *Axel Barrau*[1], *Mohammed El Badaoui*[1,2]

[1] Safran Tech, Safran SA
Rue des Jeunes Bois-Châteaufort, 78772 Magny-les-Hameaux, France
[2] Univ Lyon, UJM-St-Etienne, LASPI, EA3059, F-42023
Saint-Etienne, France

ABSTRACT

Demodulation consists in factorizing a signal as a product of a high-frequency component (carrier) and a low-frequency component (modulation). Most of the classical demodulation methods developed for telecommunications cannot be transposed directly on mechanical problems. In gearbox vibration monitoring the assumption that the carrier energy is concentrated on a single harmonic is not verified. This paper shows the limits of this assumption and proposes a new approach based on optimization, more adapted to line spectrum signals.

Index Terms— Fault diagnosis, Multi-carrier demodulation, Vibration signal, Singular Value Decomposition, Source reconstruction

1. INTRODUCTION

Gears are one of the most critical parts of mechanical systems, especially in the aeronautics industry due to both high speed rotation and heavy load of aircraft and helicopter engines. A damage lately detected in the gearbox may lead to catastrophic failure. Therefore, development of gear fault diagnosis techniques based on vibration analysis has been conducted for more than four decades [1, 2, 3].

Vibrations generated by rotating machines are usually regarded as a meaningful signature of their health state, instantaneously expressing any change in the structure or operating regime of the system [4]. Acoustic emission was recently used to detect incipiant faults in mechanical systems [5, 6, 7], but its use and interpretation become difficult in extreme measurement environment. Thus, due to easier implementation and lower signal-to-noise ratio, direct vibration measurement using accelerometers remains the standard technique for early fault detection in mechanical systems [8, 9, 10].

A major challenge of this field is isolating the signal of interest out of a global vibration resulting from several moving parts of the system under study. Much research has been carried out on the general topic of recovering a set of signals once they have been combined one way or another [11, 12, 13, 14] . This issue is not specific to mechanical systems, and actually takes its roots in telecommunications rather than in vibration analysis [15, 16]. Blind source separation in particular, where the signals to estimate are (linearly) combined in an unknown way, gave rise to an abundant literature [17, 18]. Most proposed solutions rely on the assumption that sources are statistically independent, as does for instance the widespread *Independent Component Analysis* (ICA), but they require as many sensors as sources [19]. When working with complex mechanical systems such as aircraft engines, there are typically many vibration sources and few sensors. As compensation, signals have a very structured frequency content. This is leveraged for instance by *Synchronous Average*, where the measured time series is sliced into small sequences of a given duration [20, 21, 22]. Averaging these slices then filters out the sources having a period different from the chosen duration. This procedure requires a single sensor only, which is also the case of the method we will discuss.

In the present paper we go further into using prior knowledge of the shape of the signal of interest. Vibrations produced by a spur gear have been modeled as a product of two periodic functions related to the gearboxs kinematic [23]. The issue discussed here is recovering the contributions of each function from the global signal while removing additional unwanted components. The main contribution of the paper is the formulation as an optimal reconstruction problem which, although non-quadratic, is shown to have a closedform solution based on Singular Value Decomposition (SVD). Once the separation step is performed, the status of the machine can be identified and characterized with statistical indicators (RMS, kurtosis...), spectral or cepstral analysis.

2. PROBLEM SETUP

We consider a gearbox reducer made of two wheels, wheel 1 and wheel 2, having W_1 and W_2 teeth respectively. In stationary conditions, i.e. at constant rotation speed, the gears have rotation frequencies f_1 and f_2 (Hz) respectively. The meshing frequency, which corresponds to the engagement speed between the wheels, is defined as: $f_e = W_1 \times f_{gear1} = W_2 \times f_{gear2}$. A gearbox vibration signal is usually represented as an amplitude-modulated signal [24], as in Equation (1) below:

$$s(t) = s_e(t) \times (1 + s_{gear1}(t) + s_{gear2}(t)), \tag{1}$$

where $s(t)$ is the measured signal, the first factor $s_e(t)$ is a kind of "average" gear mesh signal and the second one contains two (periodic) perturbations $s_{gear1}(t)$ and $s_{gear2}(t)$ related to angular positions of wheels 1 and 2. Of course, $s_{gear1}(t)$ has frequency f_1 and $s_{gear2}(t)$ has frequancy f_2.

When a default appears on one of the wheel teeth, the associated modulation function s_{gear1} or s_{gear2} is affected. In order to improve detection and localization of the incipiant fault, a focus is made in the present paper on the breakdown of the measured signal $s(t)$ into its gear mesh signal $s_e(t)$ and wheels components $s_{gear1}(t)$ and $s_{gear2}(t)$.

3. DECOMPOSITION OF A PRODUCT SIGNAL

In the present section, recovering signals $s_e(t)$, $s_{gear1}(t)$, $s_{gear2}(t)$ of Equation (1) from $s(t)$ is cast into the more general framework of recovering two signals $s_1(t)$ and $s_2(t)$ from their product $s(t)$:

$$s(t) = s_1(t) \times s_2(t). \tag{2}$$

This question is formulated as a non-quadratic optimisation problem and a closed-form solution is derived. Note that factor $s_2(t)$ takes here the place of $(1 + s_{gear1}(t) + s_{gear2}(t))$. This is not restrictive as $s_{gear1}(t)$ and $s_{gear2}(t)$ have separated spectral supports.

3.1. Notations

The following notations will be used:

- $s_i(t)$: Time signal, index i being 1 or 2.
- N_i, f_i, T_i, I_i: Number of harmonics, frequency and period of $s_i(t)$, I_i denoting the discrete set $[-N_i, N_i]$.
- T_{tot}, K_1, K_2: Respectively, lowest common multiple of the periods T_1 and T_2 and integers K_1 and K_2 defined by the factorizations $T_{tot} = K_1 T_1 = K_2 T_2$.
- $||\cdot||$: Modulus if applied to a complex number, or 2-norm if applied to a T_{tot}-periodic signal: $||x||^2 = \int_0^{T_{tot}} x(t)^2 dt$.
- $D(N, T)$: Set of the $T-$periodic functions whose first N harmonics at most are non-zero.
- $\hat{s}_i[k]$: k-th harmonic of the spectrum of $s_i(t)$ regarded as a T_{tot}-periodic signal (which makes sense because all signals at play have a period dividing T_{tot}). Index k can be negative.
- O_p: Set of unitary matrices of size $p \times p$.

3.2. Demodulation as an optimisation problem

Demodulation is widely used in telecommunications, where the carrier energy is usually concentrated on one harmonic. But it is easily noticed that if several harmonics are visible, then classical deconvolution, proposed by Mc Fadden in [4] and using time synchronous averages and Hilbert transform, ignores most of the available information. This case is encountered when monitoring gearbox vibrations, as the high-frequency component $s_1(t)$ stems from a meshing.

In the multi-carrier demodulation we propose, the estimated couple $(\tilde{s}_1(t), \tilde{s}_2(t))$ is defined as the solution of an optimization problem:

$$(\tilde{s}_1, \tilde{s}_2) = \underset{\substack{s_1 \in D(N_1, T_1) \\ s_2 \in D(N_2, T_2)}}{\operatorname{argmin}} \left(||s(t) - s_1(t)s_2(t)||^2 \right). \tag{3}$$

In spite of the quadratic term $s_1(t)s_2(t)$ appearing in the L_2 norm, this optimization is tractable under the hypothesis

$$2N_2 f_2 < f_1. \tag{4}$$

Proposition 1 shows it can then be reduced to a low-rank approximation problem. The result will be shown step by step using lemmas 1 and 2.

Lemma 1. *Let $C(s_1, s_2) = ||s(t) - s_1(t)s_2(t)||^2$ be the cost function appearing in Eq.* (3). *In the Fourier domain, $C(\cdot, \cdot)$ can be written as:*

$$C(\hat{s}_1, \hat{s}_2) = C_1(\hat{s}_1, \hat{s}_2) + C_2, \tag{5}$$

where C_2 is independent from $(\hat{s}_1, \hat{s}_2)$ and:

$$C_1(\hat{s}_1, \hat{s}_2) = \sum_{(i_1,i_2)\in I_1 \times I_2} ||\hat{s}[K_1 i_1 + K_2 i_2] - \hat{s}_1[K_1 i_1]\hat{s}_2[K_2 i_2]||^2 .$$

Proof. Using Parseval's theorem, we can express $C(\hat{s}_1, \hat{s}_2)$ as

$$C(\hat{s}_1, \hat{s}_2) = \sum_{i=-\infty}^{+\infty} ||\hat{s}[i] - (\hat{s}_1 * \hat{s}_2)[i]||^2 ,$$

with $\hat{s}_1 * \hat{s}_2$ the convolution product of $\hat{s}_1$ and $\hat{s}_2$: $(\hat{s}_1 * \hat{s}_2)[i] = \sum_{j=-\infty}^{+\infty} \hat{s}_1[i-j]\hat{s}_2[j]$. The value of $\hat{s}_1[i]$ (resp. $\hat{s}_2[i]$) is non-zero only for $i \in \{K_1 i_1, i_1 \in I_1\}$ (resp. $i \in \{K_2 i_2, i_2 \in I_2\}$), thus $(\hat{s}_1 * \hat{s}_2)[i]$ is non-zero only for $i \in I = \{i_1 K_1 + i_2 K_2, i_1 \in I_1, i_2 \in I_2\}$. This suggests the following decomposition:

$$C(\hat{s}_1, \hat{s}_2) = \sum_{i \in I} ||\hat{s}[i] - (\hat{s}_1 * \hat{s}_2)[i]||^2 + \sum_{i \notin I} ||\hat{s}[i]||^2 . \tag{6}$$

The second term of (6) is independent from $(\hat{s}_1, \hat{s}_2)$ and will be denoted by C_2. Let us denote by $C_1(\hat{s}_1, \hat{s}_2)$ the first term of (6). Hypothesis (4) ensures that each element of I is reached by only one combination $K_1 i_1 + K_2 i_2$ for $i_1 \in I_1$ and $i_2 \in I_2$. Thus, the sum defining $C_1(\hat{s}_1, \hat{s}_2)$ can be safely parameterized by $i_1 \in I_1$ and $i_2 \in I_2$ instead of $i \in I$: $C_1(\hat{s}_1, \hat{s}_2) = \sum_{(i_1,i_2)\in I_1 \times I_2} ||\hat{s}[K_1 i_1 + K_2 i_2] - (\hat{s}_1 * \hat{s}_2)[K_1 i_1 + K_2 i_2]||^2$. Still because of the hypothesis (4), we have: $(\hat{s}_1 * \hat{s}_2)[K_1 i_1 + K_2 i_2] = \hat{s}_1[K_1 i_1]\hat{s}_2[K_2 i_2]$ (there cannot be more than one non-zero term in the infinite sum defining $(\hat{s}_1 * \hat{s}_2)$ above). This gives the desired expression for $C_1(\hat{s}_1, \hat{s}_2)$. □

The term C_2 can be dropped when optimizing over the couple $(\hat{s}_1[\cdot], \hat{s}_2[\cdot])$. These two series consisting mostly of zeros, we introduce two column vectors $S_1 \in \mathbb{R}^{2N_1+1}$ and $S_2 \in \mathbb{R}^{2N_2+1}$ containing only the entries multiple of K_1 (resp. K_2):

$$S_1(1 + N_1 + i_1) = \hat{s}_1(K_1 i_1) \text{ for } i_1 = [-N_1, \ldots N_1],$$
$$S_2(1 + N_2 + i_2) = \hat{s}_2(K_2 i_2) \text{ for } i_2 = [-N_2, \ldots N_2].$$

This allows re-writing the optimization problem (3) under an advantageous matrix form:

Lemma 2. *The cost $C_1(\hat{s}_1, \hat{s}_2)$ of Lemma 1, written as a function of S_1 and S_2, takes the following matrix form:*

$$C_1(S_1, S_2) = \left|\left| M_S - S_1 S_2^T \right|\right|^2_{Fro}, \tag{7}$$

where $||\cdot||_{Fro}$ denotes the Frobenius norm and M_S is a $(2N_1+1) \times (2N_2+1)$ matrix defined as:

$$M_S(1 + N_1 + i_1, 1 + N_2 + i_2) = \hat{s}(K_1 i_1 + K_2 i_2). \tag{8}$$

Proof. Equation (7) is mere reordering of the terms of C_1. □

When S_1 and S_2 describe their definition domain, the product $S_1 S_2^T$ exactly describes the set of rank-one matrices. Consequently, minimizing C_1 boils down to a low-rank matrix approximation solvable by SVD-factorization:

Proposition 1. *The optimization problem* (3) *can be solved in the Fourier domain through the following steps:*

1. *Compute $\hat{s}[.]$ and build matrix M_S (Equation* (8)*).*
2. *Perform the SVD-factorization $M_S = UDV^T$, with $U \in O_{2N_1+1}$, $V \in O_{2N_2+1}$ and D a diagonal matrix.*
3. *Define $S_1 = D_{1,1}U_{:,1}$ and $S_2 = V_{:,1}$.*
4. *Use the inverse Fourier transform to retrieve $\tilde{s}_1$ and $\tilde{s}_2$.*

4. SIMULATION AND EXPERIMENTAL RESULTS

The multi-carrier demodulation method described in Proposition 1 is now applied to simulated and real signals and the results are presented in subsections 4.1 and 4.2 respectively.

4.1. Simulation

A simulated signal $s(t)$ is generated, multiplying two periodic signals $s_1(t)$ and $s_2(t)$ and adding a white gaussian noise w_t as in Equation (9) described below:

$$\begin{cases} s_1(t) = \sum_{n_1=0}^{N_1} A_{n_1} \cos(2n_1\pi f_1 t + \varphi_1), \\ s_2(t) = \sum_{n_2=0}^{N_2} A_{n_2} \cos(2n_2\pi f_2 t + \varphi_2), \\ s(t) = s_1(t) \times s_2(t) + w_t, \end{cases} \tag{9}$$

with A_{n_1} and A_{n_2} the amplitudes of the n-th harmonics and φ_1 and φ_2 the phases of $s_1(t)$ and $s_2(t)$ respectively.

For this example, the signals have frequencies $f_1 = 500Hz$ and $f_2 = 20Hz$ respectively and $N_1 = 9$ and $N_2 = 5$ harmonics, in order to be close to gearbox vibration characteristics. It has to be precised that the number of harmonics of the low-frequency function has to be chosen carefully in order to avoid the aliasing, i.e., to ensure Hypothesis (4). Figure 1 shows an example where $s_1(t)$ and $s_2(t)$ are recovered from $s(t)$, in very noisy measurement conditions (SNR=-10dB). Both high-frequency and low-frequency signals are almost perfectly reconstructed on the temporal representation.

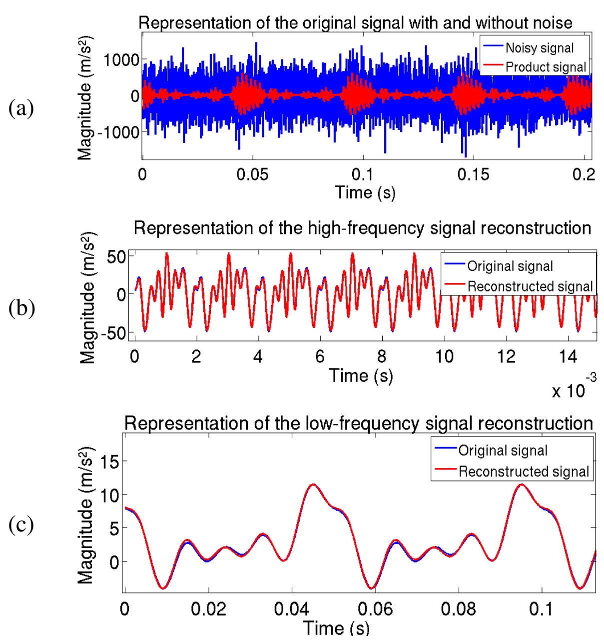

Fig. 1. Graphical representation of the simulated signal in a very noisy background (signal-to-noise ratio = -10dB). (a) represents the superposition of the noisy signal and the original product, (b) and (c) present respectively the reconstruction of the high-frequency and low-frequency signals.

In order to assess the performances of the proposed decomposition method, several Monte-Carlo simulations have been carried out. The influence of the number of parameters in the function (i.e., the number of harmonics N_1 and N_2) on the reconstruction error of the product signal has been checked. The reconstruction error Err is defined by:

$$Err = \frac{||s(t) - \tilde{s}_1(t)\tilde{s}_2(t)||^2}{||s(t)||^2} \times 100, \tag{10}$$

and plotted as a percentage.

For the first test, the number of harmonics for s_1 ranges from $N_1 = 2$ to $N_1 = 17$ and respectively for s_2 from $N_2 = 2$ to $N_2 = 11$. Figure 2 shows that the reconstruction error increases linearly whith the number of harmonics and for a given SNR, the number of harmonics deteriorates the reconstruction. It can also be noted that the error stays below 0.12% (here $SNR = 0dB$). Other signal-to-noise ratios have been tested, from $-20dB$ to $+20dB$, and the relation between the number of parameters and the reconstruction error stays approximately linear. The reconstruction error reaches 12% in the most noisy case, i.e., $SNR = -20dB$, which is widely acceptable in mechanical applications.

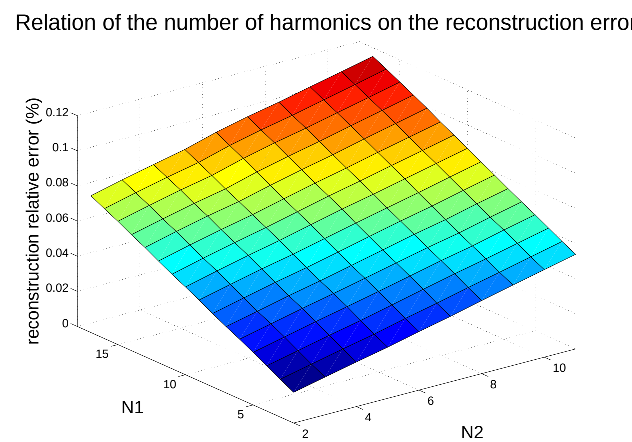

Fig. 2. Relative error of the reconstruction signal for a SNR=0dB and for several numbers of harmonics for each function.

A second test has been performed to check the influence of the signal-to-noise ratio and the number of harmonics. Figure 3 displays the average reconstruction error obtained on 1000 Monte-Carlo runs for two different settings: (a) $N_1 = 9$ while N_2 ranges from $N_2 = 2$ to $N_2 = 11$ and (b) $N_2 = 5$ while N_1 ranges from $N_1 = 2$ to $N_1 = 17$.

In both cases, the quality of the reconstruction is deteriorated with the increase of background noise and with the number of harmonics. We see that reconstruction error stays below 10% for all signal-to-noise ratios until $-25dB$, meaning the noise is correctly filtered by the method and the signals are well recovered.

4.2. Gearbox signals

We come now to the initial motivation of the proposed demodulation method. Equation (1) is commonly used in gear fault detection to model the measured vibration signal. This choice being mostly based on the empirical observation that side bands appear in the vibration spectrum around the meshing harmonics, we will challenge it applying our method to real data. The signals we used stem from a test bench instrumented by CETIM and are publicly available.

The gears have 20 and 21 teeth respectively and the measurements are made at a sampling frequency of 20 kHz. The rotation

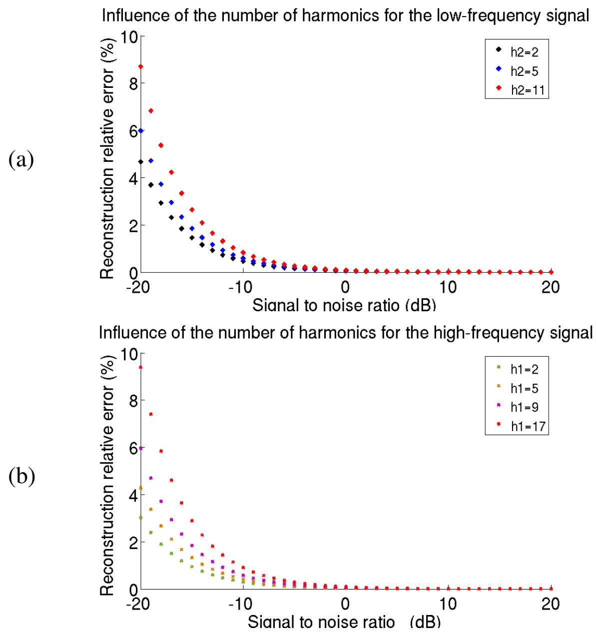

Fig. 3. Reconstruction relative error of the product function for several noisy environments. (a) represents the influence of the number of harmonics for the low-frequency function while (b) represents the influence of the high-frequency function's number of harmonics for several SNR in both case.

frequencies of gears are $f_1 = 16.75Hz$ and $f_2 = 17Hz$ respectively. To match the theoretical model of spur gear signal (Equation (1)) to Equation (2) we set $s_1(t) = s_{mesh}(t)$ and $s_2 = 1 + s_{gear1}(t) + s_{gear2}(t)$. As the frequencies of s_{gear1} and s_{gear2} are different, they are easily separated filtering s_2. In this study, the decomposition is based on 16 harmonics of the meshing signal and 8 harmonics of each gear signal. The spectra of the original signal and the reconstructed one are overlaid in Figure 4.

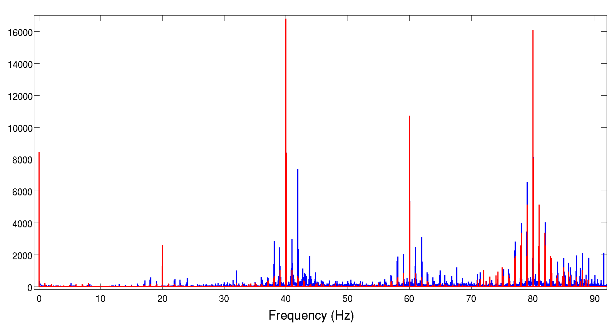

Fig. 4. Overlay of the original and reconstructed signals' spectra.

The spectrum is not fully reconstructed. We see that about half the side bands energy is captured by the product approximation (red). This can be due to the aliasing present in the gear spectrum, as in this application there is no certainty that the condition (4) is fully respected, or additional sources, and solving this question would require further investigation of the mechanical processes at play. In any case, the product hypothesis may be an interesting approximation of the signal but not its perfect representation.

To recover s_{gear1} and s_{gear2}, it is still possible to band-pass filter s_2. The outputs of the optimum decomposition are represented in Figure 5, for a sound run and for a run where a fault has been diagnosed on one gear. We see that considering each component

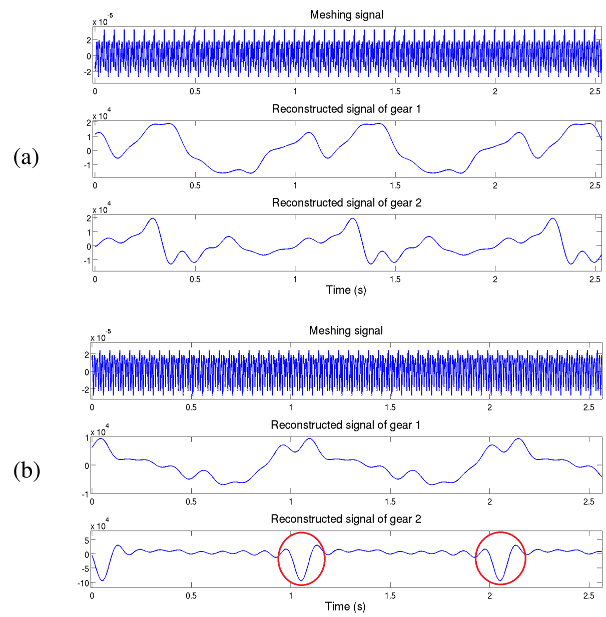

Fig. 5. Temporal representation of the reconstructed signals (meshing, gear 1 and gear 2) for a sound run (a) and a faulty run (b).

of the signal separately makes monitoring easier. When a failure appears, it becomes visible on the concerned recovered signal, as in Figure 5. Then, traditional fault indicators can be calculated directly on s_{gear1} and s_{gear2}, allowing early detection of the fault as well as its localization.

5. CONCLUSION

This paper presents a new simple approach to the issue of separating the components of a product signal measured by a single vibration sensor. The returned signals are a meaningful representation of its vibration content, and a promising tool for early diagnosis and default localization. In future work, the method will be extended to more elaborated signals, including more complex gearboxes and simultaneous amplitude and phase modulation. A study will also be carried out on using the residual signal for fault detection.

6. REFERENCES

[1] Paul D. Samuel and Darryll J. Pines, "A review of vibration-based techniques for helicopter transmission diagnostics," *Journal of Sound and Vibration*, vol. 282, no. 1-2, pp. 475–508, 2005.

[2] Mehrdad Heydarzadeh, Negin Madani, and Mehrdad Nourani, "Gearbox fault diagnosis using power spectral analysis," in *Signal Processing Systems (SiPS), 2016 IEEE International Workshop on*. IEEE, 2016, pp. 242–247.

[3] Jan Furch, Trung Tin Nguyen, and Josef Glos, "Diagnostics of gear fault in four-speed gearbox using vibration signal," in

Military Technologies (ICMT), 2017 International Conference on. IEEE, 2017, pp. 87–92.

[4] P D McFadden, "Detecting fatigue cracks in gears by amplitude and phase demodulation of the meshing vibration," *Journal of vibration, acoustics, stress, and reliability in design*, vol. 108, no. 2, pp. 165–170, 1986.

[5] Mehrdad Heydarzadeh, Mehrdad Nourani, John Hansen, and Shahin Hedayati Kia, "Non-invasive gearbox fault diagnosis using scattering transform of acoustic emission," in *Acoustics, Speech and Signal Processing (ICASSP), 2017 IEEE International Conference on*. IEEE, 2017, pp. 371–375.

[6] Yu Zhang, Wenxiu Lu, and Fulei Chu, "Planet gear fault localization for wind turbine gearbox using acoustic emission signals," *Renewable Energy*, vol. 109, pp. 449–460, 2017.

[7] Linghao Zhou, Fang Duan, David Mba, and Elasha Faris, "A comparative study of helicopter planetary bearing diagnosis with vibration and acoustic emission data," in *Prognostics and Health Management (ICPHM), 2017 IEEE International Conference on*. IEEE, 2017, pp. 246–251.

[8] Matthew Greaves, "Towards the next generation of HUMS sensor," *ISASI 2014 Seminar*, vol. 1, no. October, pp. 1–13, 2014.

[9] Zhipeng Feng, Xuefeng Lin, and Ming J. Zuo, "Joint amplitude and frequency demodulation analysis based on intrinsic time-scale decomposition for planetary gearbox fault diagnosis," *Mechanical Systems and Signal Processing*, vol. 72-73, pp. 223–240, 2016.

[10] Dan He, Xiufeng Wang, Shancang Li, Jing Lin, and Ming Zhao, "Identification of multiple faults in rotating machinery based on minimum entropy deconvolution combined with spectral kurtosis," *Mechanical Systems and Signal Processing*, vol. 81, pp. 235–249, 2016.

[11] P. D. McFadden and J. D. Smith, "A signal processing technique for detecting local defects in a gear from the signal average," *Proceedings of the Institution of Mechanical Engineers, Part C: Journal of Mechanical Engineering Science*, vol. 199, pp. 287–292, 1985.

[12] M.J. Roan, J.G. Erling, and L.H. Sibul, "A new, non-linear, adaptive, blind source separation approach to gear tooth failure detection and analysis," *Mechanical Systems and Signal Processing*, vol. 16, no. 5, pp. 719 – 740, 2002.

[13] Khalid Sabri, Mohamed El Badaoui, François Guillet, Abdellah Adib, and Driss Aboutajdine, "Gear signal separation by exploiting the spectral diversity and cyclostaionarity," in *Acoustics, Speech and Signal Processing, 2006. ICASSP 2006 Proceedings. 2006 IEEE International Conference on*. IEEE, 2006, vol. 3, pp. III–III.

[14] GD Elia, M Cocconcelli, E Mucchi, and G Dalpiaz, "Combining blind separation and cyclostationary techniques for monitoring distributed wear in gearbox rolling bearings," *Proceedings of the Institution of Mechanical Engineers, Part C: Journal of Mechanical Engineering Science*, vol. 231, no. 6, pp. 1113–1128, 2017.

[15] John AC Bingham, "Multicarrier modulation for data transmission: An idea whose time has come," *IEEE Communications magazine*, vol. 28, no. 5, pp. 5–14, 1990.

[16] Zhimin Chen, Lenan Wu, and Peng Chen, "Efficient modulation and demodulation methods for multi-carrier communication," *IET Communications*, vol. 10, no. 5, pp. 567–576, 2016.

[17] Adel Belouchrani, Karim Abed-Meraim, J-F Cardoso, and Eric Moulines, "A blind source separation technique using second-order statistics," *IEEE Transactions on signal processing*, vol. 45, no. 2, pp. 434–444, 1997.

[18] C. Servière and P. Fabry, "Blind source separation of noisy harmonic signals for rotating machine diagnosis," *Journal of Sound and Vibration*, vol. 272, pp. 317–339, 2004.

[19] Fang Duan, Michael Corsar, Linghao Zhou, and David Mba, "Using independent component analysis scheme for helicopter main gearbox bearing defect identification," in *Prognostics and Health Management (ICPHM), 2017 IEEE International Conference on*. IEEE, 2017, pp. 252–259.

[20] P. D. McFadden, "A technique for calculating the time domain averages of the vibration of the individual planet gears and the sun gear in an epicyclic gearbox," *Journal of Sound and Vibration*, vol. 144, no. 1, pp. 163–172, 1991.

[21] Zhile Wang, Yu Guo, and Xing Wu, "Sun gear fault diagnosis based on windowed synchronous average in angle domain," in *Information and Automation (ICIA), 2016 IEEE International Conference on*. IEEE, 2016, pp. 785–790.

[22] Lei Zhao, Yu Guo, and Xing Wu, "Investigation on synchronous averaging for fault feature extraction of sun gear in a planetary gearbox," in *Applied System Innovation (ICASI), 2017 International Conference on*. IEEE, 2017, pp. 1383–1386.

[23] William D Mark, "Analysis of the vibration excitation of of gear systems: Basic theory," *Journal of Acoustical Society of America*, vol. 63, pp. 1409–1430, 1977.

[24] Cécile Capdessus, *Aide au diagnostic des machines tournantes par traitement du signal (Aid to the diagnosis of rotating machines by signal processing)*, Ph.D. thesis, 1992.